

Chapter 4

Preparation and Characterization of $(1-x) \text{Ba}_{0.8}\text{Sr}_{0.2}\text{TiO}_3-x\text{PbTiO}_3$ Solid Solution

4.1 Introduction

Lead titanate has a tetragonal structure with a fairly high aspect ratio of 1.06 and is ferroelectric at room temperature. The transition from the cubic paraelectric phase to the ferroelectric tetragonal phase occurs at 490°C (6). Therefore, an addition of PbTiO_3 to $\text{Ba}_{0.8}\text{Sr}_{0.2}\text{TiO}_3$ will change the dielectric constant at room temperature and the Curie temperature is expected to increase.

The materials used PbO as a constituent in composition indicate an increasing weight loss and density (1). Because of its volatility above 800°C and evaporation of phase deposition, PbO must be retained during sintering at temperature up to 1300°C and limited an access to the atmosphere to prevent the loss of PbO . Despite this protection, there is normally a few percent loss of the initial PbO content which is compensated by an excess addition to the starting materials.

The dielectric properties of PbTiO_3 had been studied from many researchers. They found that lead could be substituted for barium titanate and shifted the Curie point to a higher temperature and lowered the second transition temperature. In addition, it increased the temperature range within which the variation of dielectric constant with temperature was small. But it decreased the maximum dielectric constant due to a low dielectric constant of PbTiO_3 . Lead is usually used to increase the Curie temperature of BaTiO_3 or other ferroelectric materials.

The preparation of $(\text{Pb}_x\text{Ba}_{0.5-x}\text{Sr}_{0.5})\text{TiO}_3$ solid solution was prepared by Ganesh and Goo (16). In their preparation directly from oxides and carbonates, all materials were mixed in a ball-mill for 5 hours in deionized water, following by calcining at 850°C for 5 to 8 hours. The calcined residue was ground and pressed to disks. The compacts were sintered at 1300°C for 5 hours. The increasing of lead affected the microstructure of $(\text{Pb}_x\text{Ba}_{0.5-x}\text{Sr}_{0.5})\text{TiO}_3$ which related to the dielectric properties. As the lead molar fraction of x increased, the Curie temperature increased and the dielectric constant decreased. This results from the decrease of Ba content, which effected to a lower dielectric maximum and a broadening peak.

Ganesh and Goo's work (16) showed that the crystal structures of $(\text{Pb}_x\text{Ba}_{0.5-x}\text{Sr}_{0.5})\text{TiO}_3$ were cubic structure at room temperature for $x=0, 0.1$ and 0.2 compositions and tetragonal structure for $x=0.3, 0.4$ and 0.5 compositions. The results are shown in Table 9.

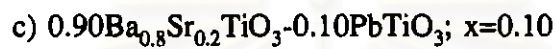
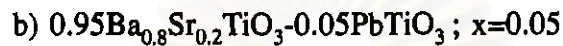
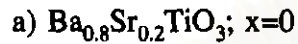
Table 9 Properties of the $\text{Pb}_x\text{Ba}_{0.5-x}\text{Sr}_{0.5}\text{TiO}_3$ system (16)

x	Lattice parameter (A°)	Crystal structure	Grain size (μm)	%theoretical density	Maximum Dielectric Constant
0.0	a = 3.947	Cubic	4.3	98	11500
0.1	a = 3.951	Cubic	4.3	96	6500
0.2	a = 3.952	Cubic	4.4	98	5800
0.3	a = 3.941 c = 3.950	Tetragonal	4.2	98	2700
0.4	a = 3.932 c = 3.953	Tetragonal	4.3	95	1650
0.5	a = 3.896 c = 3.961	Tetragonal	4.1	97	Not measurement

From the data in Table 9, the lattice constants of a decreases and c increases for tetragonal structure as lead content is increased.

4.2 Preparation

All compositions were prepared by mixing and calcining all oxides and carbonates. The compositions studied in the system of $(1-x)\text{Ba}_{0.8}\text{Sr}_{0.2}\text{TiO}_3-x\text{PbTiO}_3$ were



Pb doped BST solid solution was prepared by conventional processing techniques. Stoichiometric amounts of the chemically pure barium carbonate (99.9%), strontium carbonate (99.9%), lead oxide (99%) and titanium dioxide (99%) were weighed and wet ball-milled with ZrO_2 grinding media and ethyl alcohol as a solvent for 6 hours. After drying, the mixtures were characterized by DTA to determine the calcined temperature at which the complete reaction occurred. The measurement was taken with a heating rate of $10^\circ\text{C}/\text{min}$. From DTA data for both of before and after calcining shown in Fig 4.1, the reaction completed at 1025°C for Pb doped $\text{Ba}_{0.8}\text{Sr}_{0.2}\text{TiO}_3$.

Thus the mixture of these compositions was calcined at 1050°C with a heating rate of $2^\circ\text{C}/\text{min}$ in oxygen, and soaked at this temperature for 2 hours. To determine the remaining reaction the calcined powder was retested by DTA. The result in Fig. 4.1 showed that there were no peaks appeared indicating the complete reaction. Then the calcined materials were milled and 2% by weight of PVA were added in the last hour of milling. The powder which had been sieved through a 100-mesh screen was pressed into a disk by a single action with a pressure of 80-85 MPa.

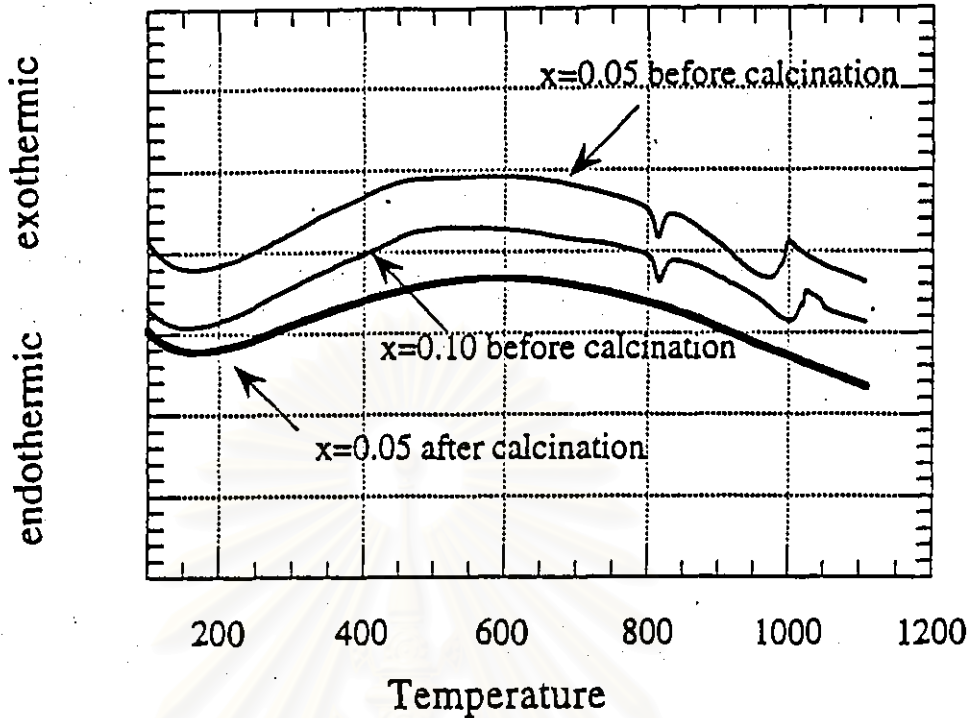


Fig. 4.1 DTA curves of $(1-x)\text{Ba}_{0.8}\text{Sr}_{0.2}\text{TiO}_3-x\text{PbTiO}_3$ before and after calcination

After burning-out binder with a heating rate of $1^\circ\text{C}/\text{min}$ and holding at 550°C for 60 minutes in oxygen, the disks were weighed before and after firing to determine the weight loss. All those compositions were sintered with a heating rate of $4^\circ\text{C}/\text{min}$ and hour soaking period at the sintering temperature, and then they were cooled in the furnace.

The structure, microstructure and dielectric properties of these compositions were characterized by XRD, SEM and Impedance Analyzer. A procedure for the measurement could be found in the previous chapter.

4.3 Results and Discussion

4.3.1 X-Ray Analysis

The crystal structure of Pb doped $\text{Ba}_{0.8}\text{Sr}_{0.2}\text{TiO}_3$ was studied. A series of XRD patterns for the samples are presented in Fig. 4.2. The results in Fig 4.2(a)

showed only single phase for both of 5% and 10% Pb-doped- $\text{Ba}_{0.8}\text{Sr}_{0.2}\text{TiO}_3$. When the amount of Pb is increased, the splitting of (002) and (200) peak representing a tetragonal phase can be seen clearly in Fig 4.2(b). The results of XRD pattern are used to compute the lattice constants of Pb doped $\text{Ba}_{0.8}\text{Sr}_{0.2}\text{TiO}_3$ as listed in Table 10.

Table 10 Structure parameters of calcined $(1-x)\text{Ba}_{0.8}\text{Sr}_{0.2}\text{TiO}_3-x\text{PbTiO}_3$ powders

Strontium molar fraction (x)	Lattice constant (\AA)	c/a ratio	X-ray density
0	a=3.990	-	5.84
0.05	a=3.988 c=4.008	1.005	6.34
0.10	a=3.986 c=4.022	1.009	6.01

From Table 10, the lattice constant of c increases with the molar fraction of Pb is increased. The lattice parameters of the powder without lead are 3.990 \AA and 4.002 \AA . For $x=0.05$, the lattice constants are 3.988 \AA and 4.008 \AA , and for $x=0.10$ they change to 3.986 \AA and 4.022 \AA , respectively. They show the decreasing of a and increasing of c constant which effect to the aspect ratio. These results imply that the crystals tend to be more anisotropic as Pb content increases.

สถาบันวิทยบริการ
จุฬาลงกรณ์มหาวิทยาลัย

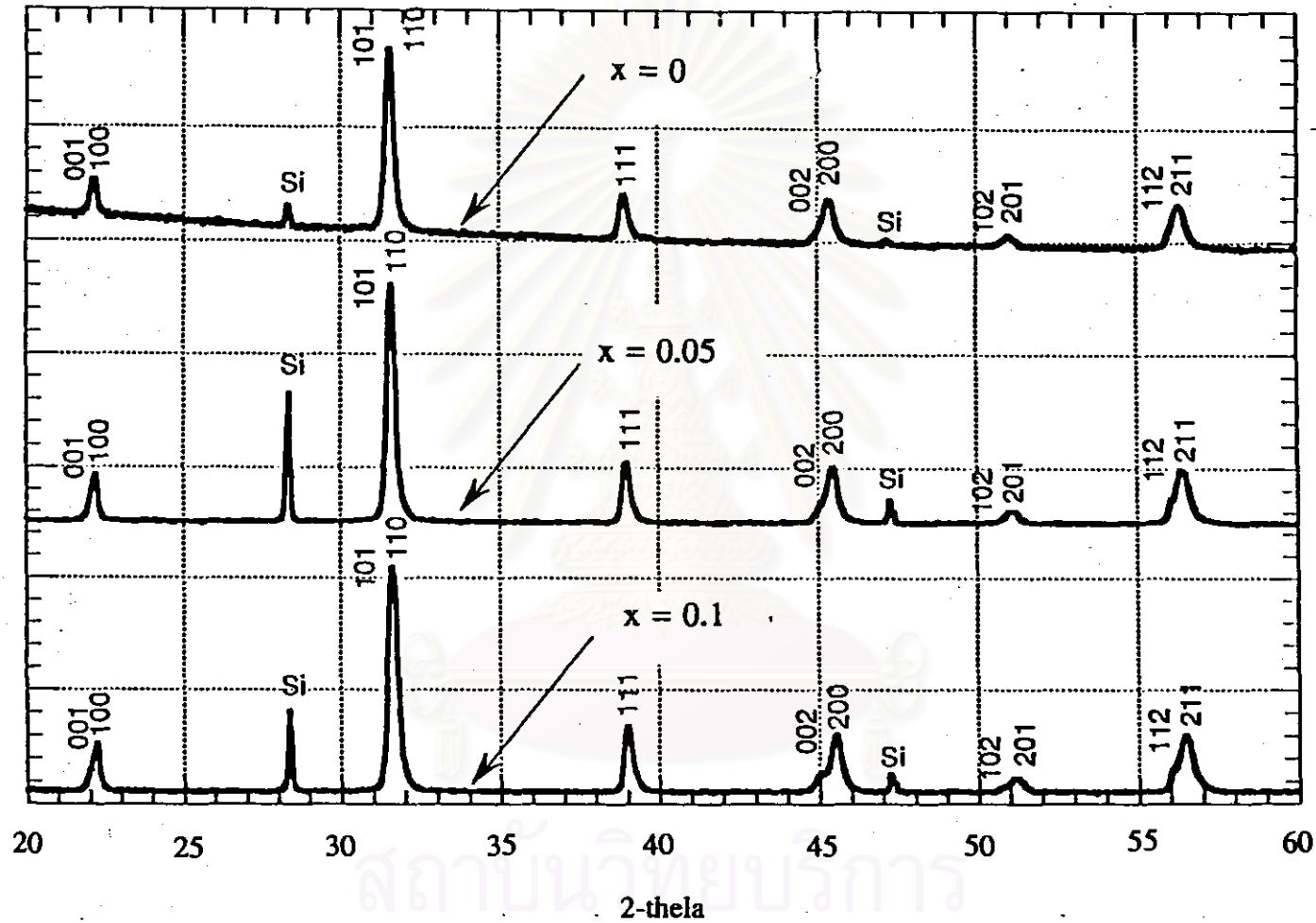


Fig. 4.2(a) XRD pattern of $(1-x)\text{Ba}_{0.8}\text{Sr}_{0.2}\text{TiO}_3-x\text{PbTiO}_3$ for $20^\circ \leq 2\theta \leq 60^\circ$

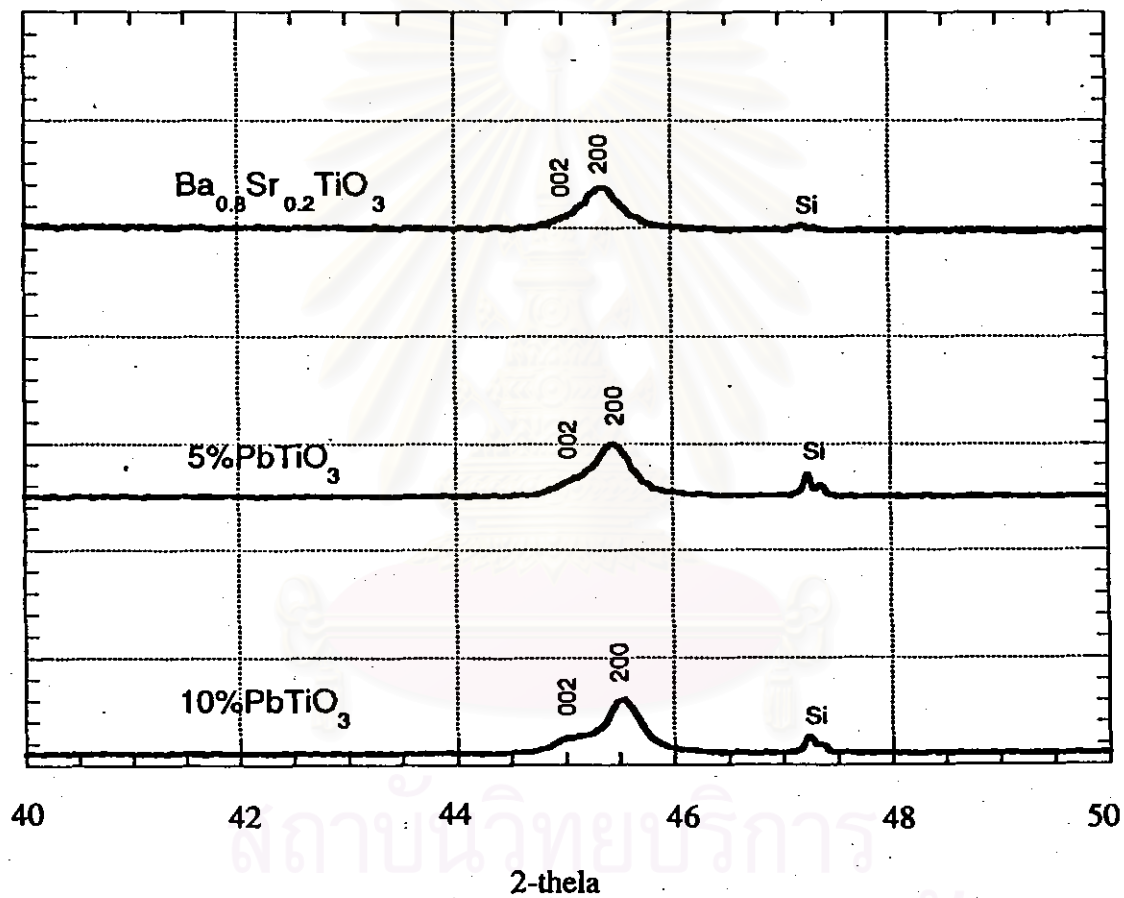
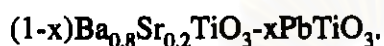


Fig. 4.2(b) XRD pattern of $(1-x)\text{Ba}_{0.8}\text{Sr}_{0.2}\text{TiO}_3-x\text{PbTiO}_3$ for $40^\circ \leq 2\theta \leq 50^\circ$

4.3.2 Weight Loss and Density After Sintering

Weight loss and density of $(1-x) \text{Ba}_{0.8}\text{Sr}_{0.2}\text{TiO}_3 - x \text{PbTiO}_3$ as a function of firing temperature are shown in Table 11.

Table 11 Weight loss and Density versus sintering temperature of



Sample	Sintering temperature (°C)	%Weight loss	%Theoretical density
$\text{Ba}_{0.8}\text{Sr}_{0.2}\text{TiO}_3$	1350	1.2	97
$0.95\text{Ba}_{0.8}\text{Sr}_{0.2}\text{TiO}_3 - 0.05\text{PbTiO}_3$	1320	2.2	94
	1350	2.6	94
$0.90\text{Ba}_{0.8}\text{Sr}_{0.2}\text{TiO}_3 - 0.10\text{PbTiO}_3$	1320	5.6	94
	1350	6.2	95

The weight loss of $\text{Ba}_{0.8}\text{Sr}_{0.2}\text{TiO}_3$ is lower than that of Pb doped $\text{Ba}_{0.8}\text{Sr}_{0.2}\text{TiO}_3$, and the weight loss increases as a function of increasing amount of Pb as indicated in Table 11. This is probably caused by the volatilization of Pb from the material. Without lead, the weight loss is 1.2 at sintering temperature of 1350°C and soaked for 30 minutes. As the molar fraction of Pb increases to 0.05 and 0.10, the weight loss also increases to 2.6 and 6.2, respectively. These results are argued that the volatilization of Pb is increased with the increasing amount of Pb and affects the increasing of weight loss. Especially, the weight loss of $x=0.10$ is too high because during sintering in flowing oxygen the sample is not in a closed crucible to prevent the oxygen vacancy existing in the sample.

The results of weight loss depend on sintering temperature as shown in Table 11. At a higher sintering temperature the weight loss of the composition tends to increase. Its value for $0.95\text{Ba}_{0.8}\text{Sr}_{0.2}\text{TiO}_3 - 0.05\text{PbTiO}_3$ is 2.2 at 1320°C and

increases to 2.6 at 1350°C. Similarly, for $0.90\text{Ba}_{0.8}\text{Sr}_{0.2}\text{TiO}_3-0.10\text{PbTiO}_3$ it increases from 5.6 at 1320 °C to 6.2 at 1350 °C. In addition, the longer soaking time affects on the increasing weight loss due to more time available for volatilization of Pb.

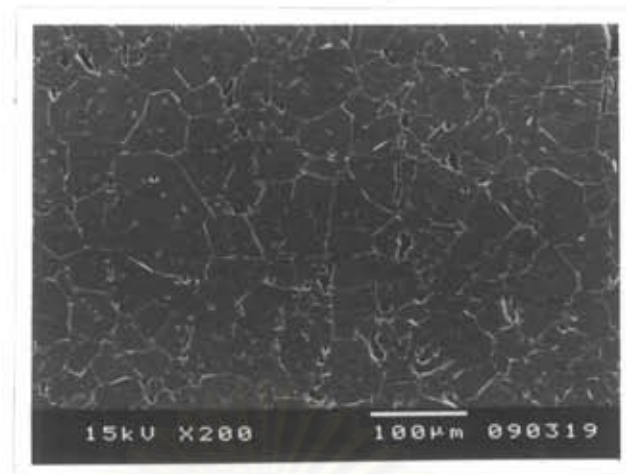
The density of Pb doped BST is approximately 93-95%, which is higher than that of undoped BST as shown in Table 11. This implies that Pb can reduce the sintering temperature. Furthermore, the densification depend on sintering temperature and soaking times and liquid phase increases as a higher sintering temperature and longer soaking time are employed.

These results indicate that the trend of density increases as Pb content is increased which is similar to the results of SEM as explained in following investigation.

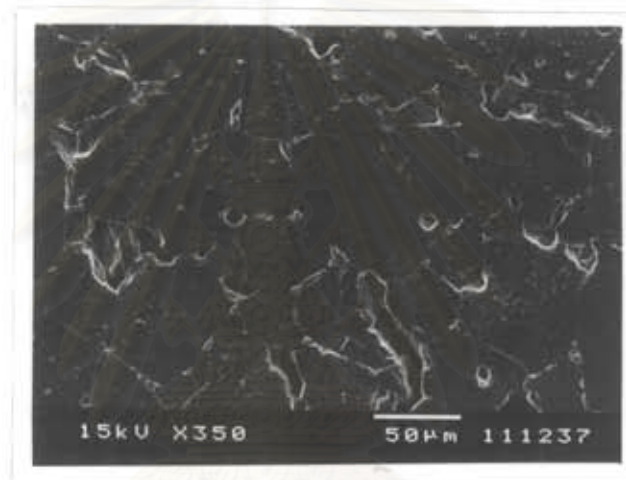
4.3.3 Microstructure

SEM micrographs of Pb doped $\text{Ba}_{0.8}\text{Sr}_{0.2}\text{TiO}_3$ in Fig.4.4 show the grain growth as the Pb content is increased. 5%Pb doped $\text{Ba}_{0.8}\text{Sr}_{0.2}\text{TiO}_3$ shows the closing of grains that grain boundary decreases which eliminates intergranular pores. The grain size increases as the Pb content is increased from 5%Pb to 10%Pb.

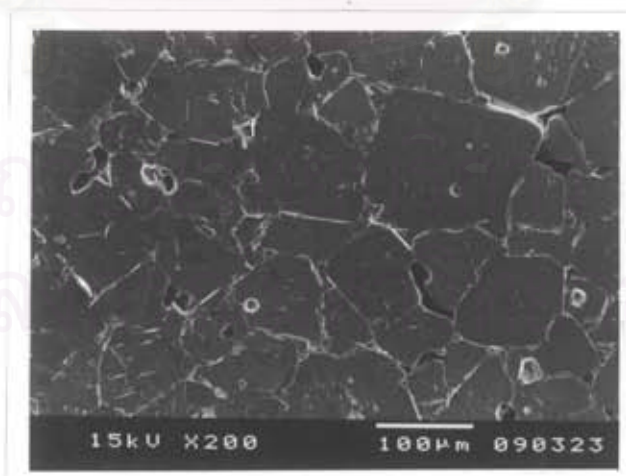
Fig. 4.5-4.6 show the increasing of grain growth when the sintering temperature and soaking time are increased. The grain growth can eliminate a partial intergranular pores and intragranular pores. The comparison of Pb doped $\text{Ba}_{0.8}\text{Sr}_{0.2}\text{TiO}_3$ is displayed that the increasing of grain growth and densification of lead doped BST are better than that of undoped BST, which is caused by the liquid phase sintering.



(a)



(b)

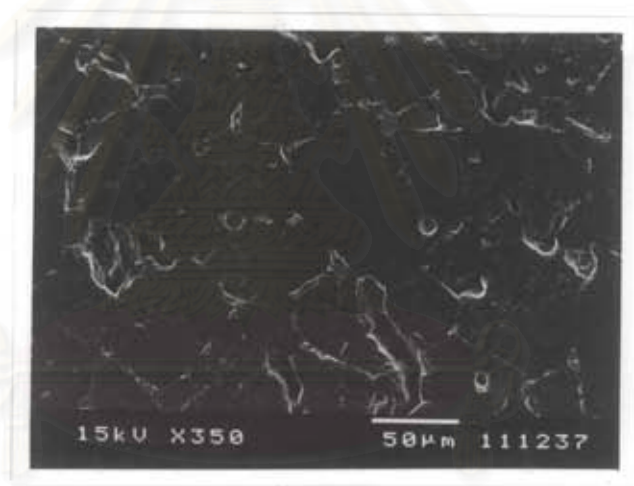


(c)

Fig. 4.3 SEM micrographs of $(1-x)\text{Ba}_{0.8}\text{Sr}_{0.2}\text{TiO}_3-x\text{PbTiO}_3$ sintered at 1350°C and soaked for 30 minutes. a) $x=0$ b) $x=0.05$ c) $x=0.10$



(a)



(b)

Fig. 4.4(a) SEM micrographs of $0.95\text{Ba}_{0.8}\text{Sr}_{0.2}\text{TiO}_3-0.05\text{PbTiO}_3$ at different sintering temperature and holding for 30 minutes a) 1320°C b) 1350°C

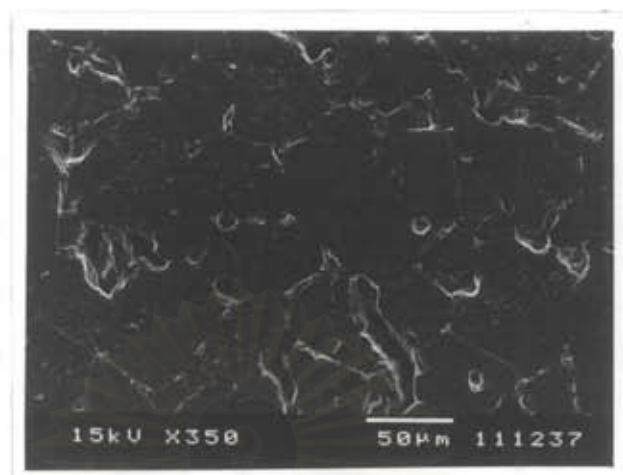


(a)

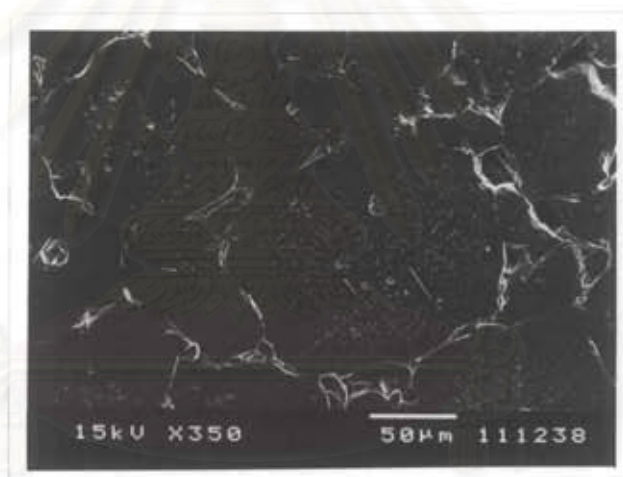


(b)

Fig. 4.4(b) SEM micrographs of $0.90\text{Ba}_{0.8}\text{Sr}_{0.2}\text{TiO}_3-0.10\text{PbTiO}_3$ at different sintering temperature and holding for 30 minutes a) 1320°C b) 1350°C



(a)



(b)

Fig. 4.5 SEM micrographs of $0.95\text{Ba}_{0.8}\text{Sr}_{0.2}\text{TiO}_3-0.05\text{PbTiO}_3$ sintered at 1350°C with different soaking time a) 30 minutes b) 1 hour

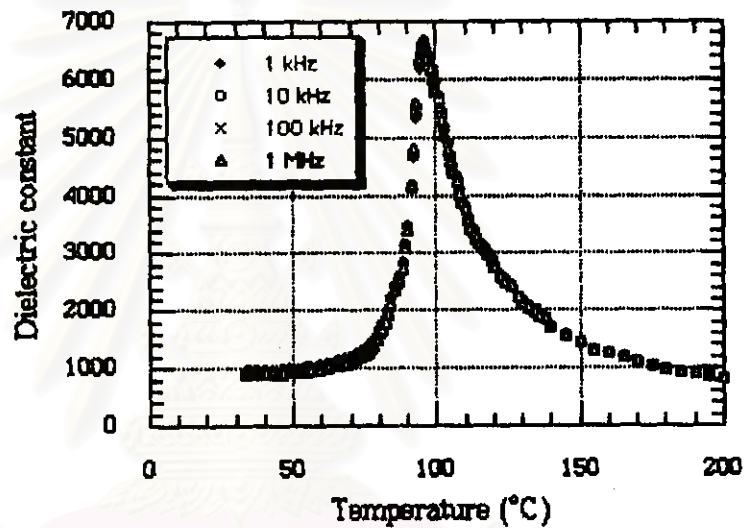
4.3.4 Dielectric Properties

Fig. 4.6 shows the effect of frequency on the dielectric constant and dissipation factor of $0.95\text{Ba}_{0.8}\text{Sr}_{0.2}\text{TiO}_3\text{-}0.05\text{PbTiO}_3$. The result shows a Curie point at 95°C and a maximum dielectric constant is about 6800. The frequency has a little effect on the dielectric constant. The shape of dielectric constant and dissipation factor for Pb doped $\text{Ba}_{0.8}\text{Sr}_{0.2}\text{TiO}_3$ are similar to undoped $\text{Ba}_{0.8}\text{Sr}_{0.2}\text{TiO}_3$, but the Curie temperature and dielectric maxima are different. The Curie point of composition with Pb dopant shifts to a higher temperature and the dielectric constant drops to lower values.

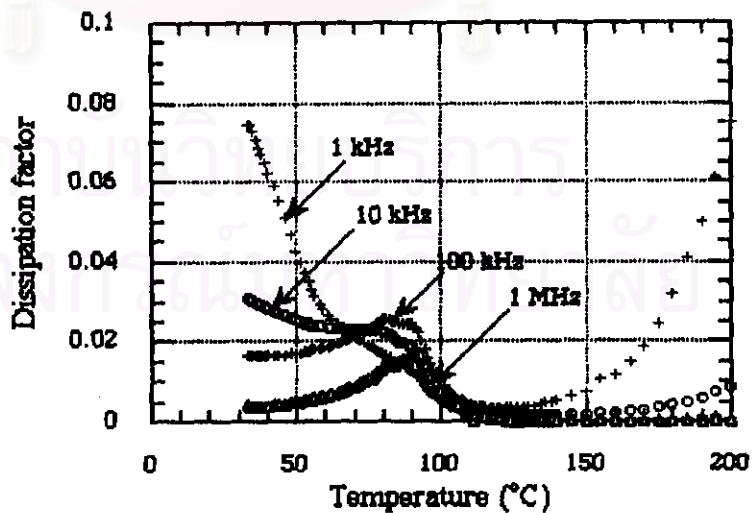
Fig. 4.7 shows the dependence of temperature on the dielectric constant and dissipation factor of $\text{Ba}_{0.8}\text{Sr}_{0.2}\text{TiO}_3$ doped with a different amount of Pb. As the Pb content increases, the Curie temperature tends to increase from 96°C for 5%Pb to 112°C for 10%Pb doped $\text{Ba}_{0.8}\text{Sr}_{0.2}\text{TiO}_3$. The dielectric constant at room temperature decreases from 2700 to 1000 as 5%Pb are doped into $\text{Ba}_{0.8}\text{Sr}_{0.2}\text{TiO}_3$. Also, the dissipation factor of compositions with Pb dopant reduces. The dissipation factor of $\text{Ba}_{0.8}\text{Sr}_{0.2}\text{TiO}_3$, at room temperature is about 0.043 and decreases to 0.025 and 0.014 for 5%Pb doped and 10%Pb doped, respectively. The decreasing of dissipation factor below the Curie point is argued that the decreasing of domain wall motion.

Pb can give a broad phase transition. This is because the substitution of Pb in Ba and Sr of A-site encourages the broad phase transition and the dielectric constant of PbTiO_3 itself is much lower than $\text{Ba}_{0.8}\text{Sr}_{0.2}\text{TiO}_3$. Nevertheless, the substitution of Pb increases anisotropic crystal structure as they cool below their Curie point which probable affects the broadening of the peak.

Fig 4.8 shows the dielectric constant as a function of temperature of 5% and 10%PbTiO₃ doped Ba_{0.8}Sr_{0.2}TiO₃ sintered at 1320 °C and 1350 °C and soaked for 30 minutes. The Curie temperature does not vary as the sintering temperature increases from 1320 °C to 1350 °C, but the maximum dielectric constant is different since the larger grains obtained from higher sintering temperature result in lower dielectric constant as shown in SEM micrograph of Fig 4.4.



(a)



(b)

Fig 4.6 Change in dielectric constant and dissipation factor at different frequencies of 5%Pb-doped Ba_{0.8}Sr_{0.2}TiO₃ sintered at 1320 °C and soaked for 30 minutes.

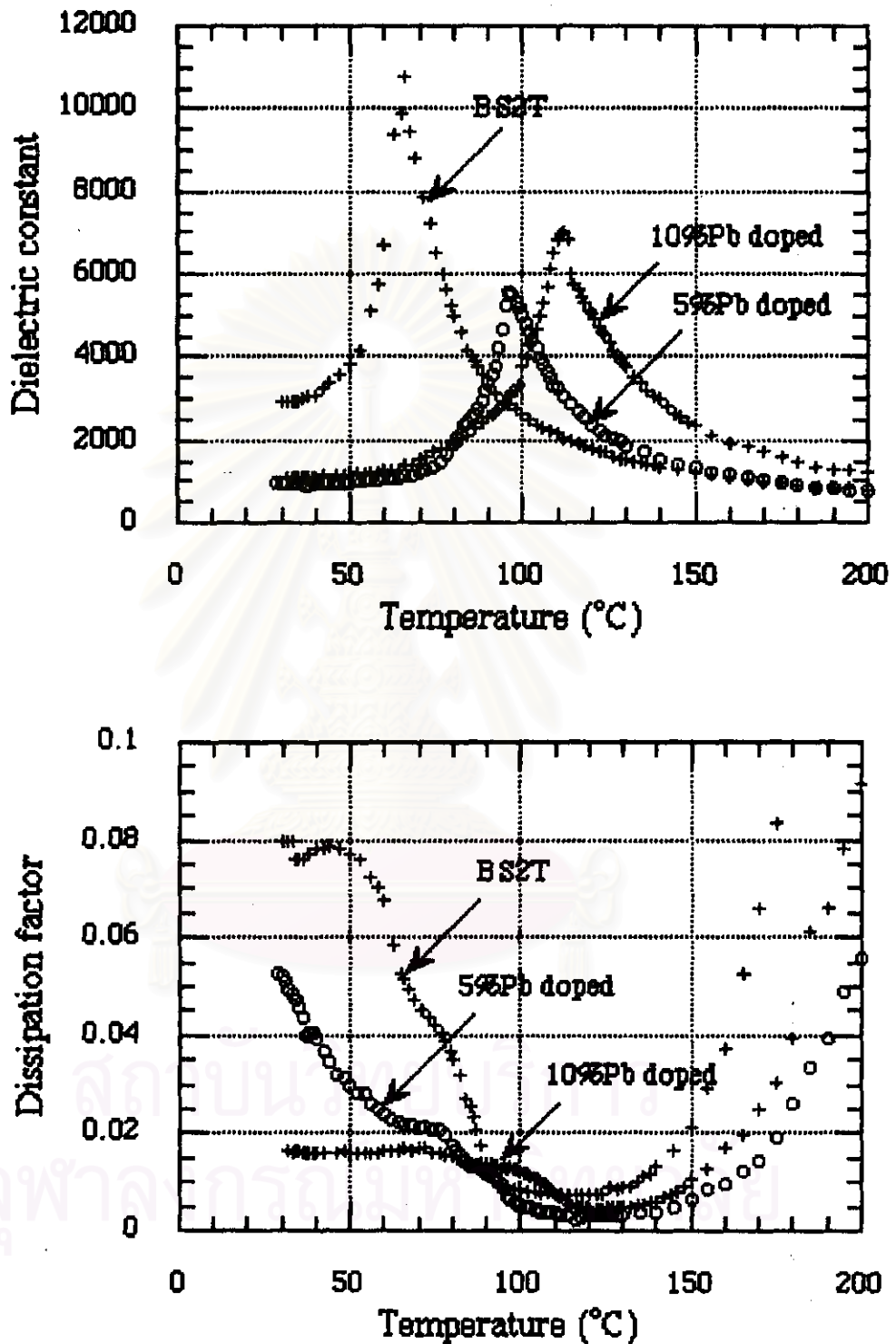


Fig 4.7 Change in dielectric constant and dissipation factor of $(1-x)\text{Ba}_{0.8}\text{Sr}_{0.2}\text{TiO}_3-x\text{PbTiO}_3$ sintered at 1350°C and soaked for 30 minutes.

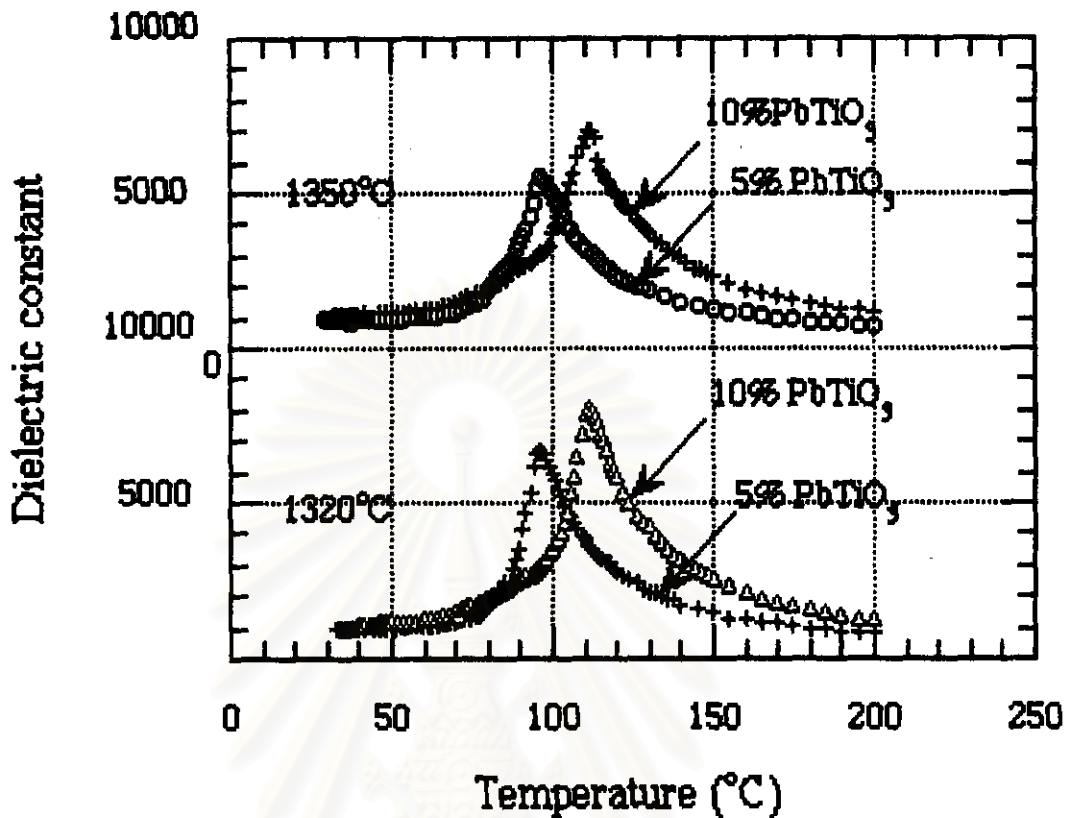


Fig 4.8 Change in dielectric constant of 5%PbTiO₃ and 10%PbTiO₃ doped

$Ba_{0.8}Sr_{0.2}TiO_3$ at different sintering temperature and soaked for 30 minutes.

Fig 4.9 shows the dielectric constant and the dissipation factor of 5%Pb doped $Ba_{0.8}Sr_{0.2}TiO_3$ with the different soaking times. The Curie point does not vary as the soaking time is increased, but the maximum dielectric constant decreases. This is probably come from grain growth and the variations of the compositional structure in the sample. In addition, the trend of the dielectric constant decreases as soaking time is increased, because of the increasing grain growth as the main factor. The dissipation factors at below Curie point decrease as the soaking time is increased which is maybe affected from the decreasing of domain wall motion.

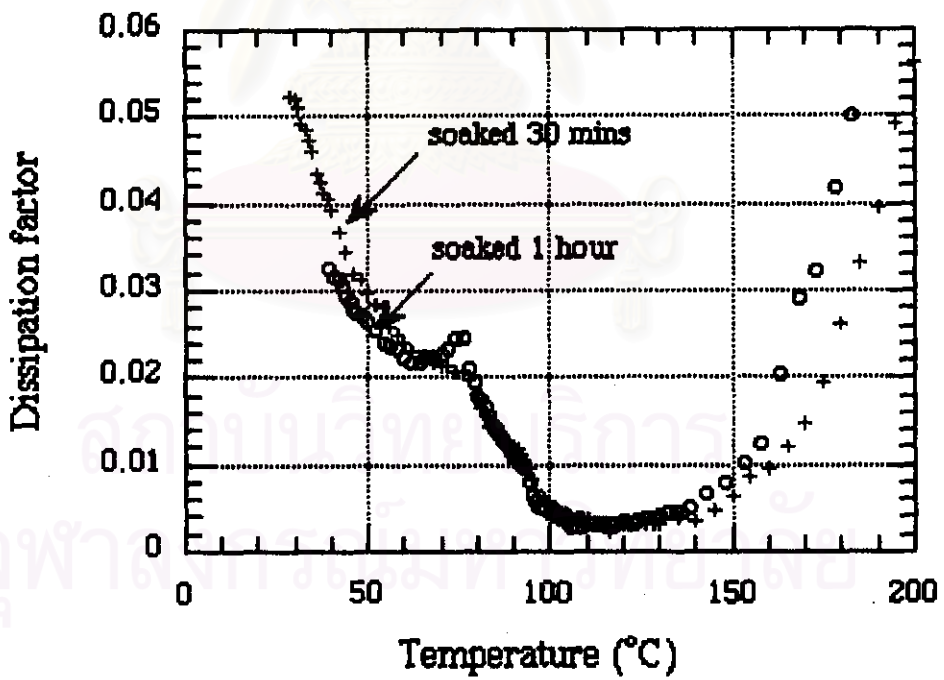
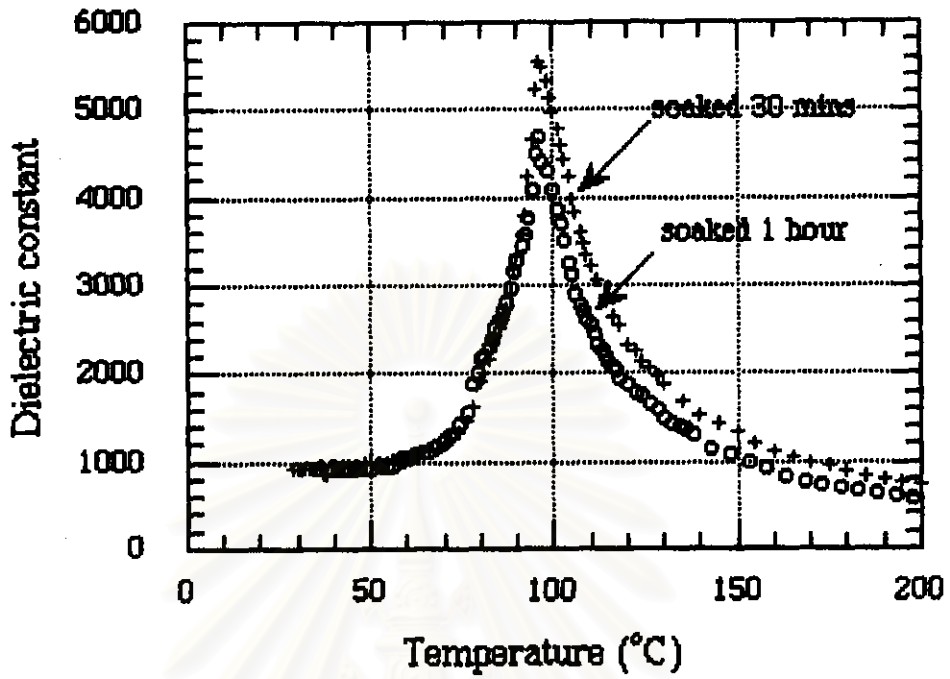
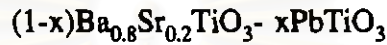


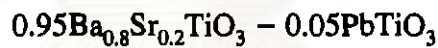
Fig 4.9 Change in dielectric constant and the dissipation factor of 5%Pb doped $\text{Ba}_{0.8}\text{Sr}_{0.2}\text{TiO}_3$ sintered at 1350°C with different soaking time.

The maximum dielectric constant as a function of composition, sintering temperature and soaking time are summarized in Table 12.

Table 12 Dielectric constant as a function of composition, sintering temperature and soaking time.



Composition (x)	Sintering temperature ($^{\circ}\text{C}$) with 30 min soaking time	Maximum dielectric constant
0	1350	10805
0.05	1320	6687
	1350	5546
0.10	1320	8036
	1350	7012



Sintering temperature ($^{\circ}\text{C}$)	Soaking time (min)	Maximum dielectric
1350	30	5546
	60	4699

These results indicate that the compositions substituted with PbTiO_3 have a diffuse phase transition, which is probably caused by inhomogeneity on microscopic scale within individual crystals. Nevertheless, the addition of lead affects the decreasing of dielectric constant at room temperature.

4.3.5 Thermal Expansion Coefficient

The results of thermal expansion for $(1-x)\text{Ba}_{0.8}\text{Sr}_{0.2}\text{TiO}_3 - x\text{PbTiO}_3$ where $x=0$ and 0.05 compositions with sintering temperature of 1350°C and soaked for 30 minutes are shown in Fig 4.10. The change of slope for Pb doped $\text{Ba}_{0.8}\text{Sr}_{0.2}\text{TiO}_3$

indicates that the turning point shifts to about 75°C which is different from the Curie point of dielectric data. The difference between the turning point of COE and the Curie point from dielectric data is about 15°C because of the effect of heating rate for using in each measurement ($1^{\circ}\text{C}/\text{min}$ for dielectric measurement and $2^{\circ}\text{C}/\text{min}$ for COE measurement) and the position of thermocouple. In addition, the change of phase transition temperature occurs at higher temperature when the larger amount of Pb is added.

Fig 4.11 shows the thermal expansion for $0.95\text{Ba}_{0.8}\text{Sr}_{0.2}\text{TiO}_3 - 0.05\text{PbTiO}_3$ sintered at 1350°C with the different soaking times. It indicates that the soaking time does not effect the change of transition temperature but it does for COE at turning point.

Table 13 shows the thermal expansion coefficient above Curie point of Pb doped $\text{Ba}_{0.8}\text{Sr}_{0.2}\text{TiO}_3$ as a function of composition, sintering temperature and soaking time. The C.O.E. value above the Curie point of $\text{Ba}_{0.8}\text{Sr}_{0.2}\text{TiO}_3$ with Pb dopant up to 10% are the same. The C.O.E. above Curie point of undoped $\text{Ba}_{0.8}\text{Sr}_{0.2}\text{TiO}_3$ is about $8.2 \times 10^{-6}/1^{\circ}\text{C}$ and changes to $8.0 \times 10^{-6}/1^{\circ}\text{C}$ for 5%PbTiO₃ doped $\text{Ba}_{0.8}\text{Sr}_{0.2}\text{TiO}_3$. When Pb increases to 10% the C.O.E. above Curie point is about $8.1 \times 10^{-6}/1^{\circ}\text{C}$. The increasing of sintering temperature from 1320°C to 1350°C is a little effect on C.O.E. value for 5%PbTiO₃ doped $\text{Ba}_{0.8}\text{Sr}_{0.2}\text{TiO}_3$ and no effect for 10%Pb doped composition. The trend of C.O.E. increases as the soaking time increases. For 5% PbTiO₃ doped $\text{Ba}_{0.8}\text{Sr}_{0.2}\text{TiO}_3$, the C.O.E. value increases from $8.0 \times 10^{-6}/1^{\circ}\text{C}$ to $8.3 \times 10^{-6}/1^{\circ}\text{C}$ when the soaking time increases from 30 minutes to a hour.

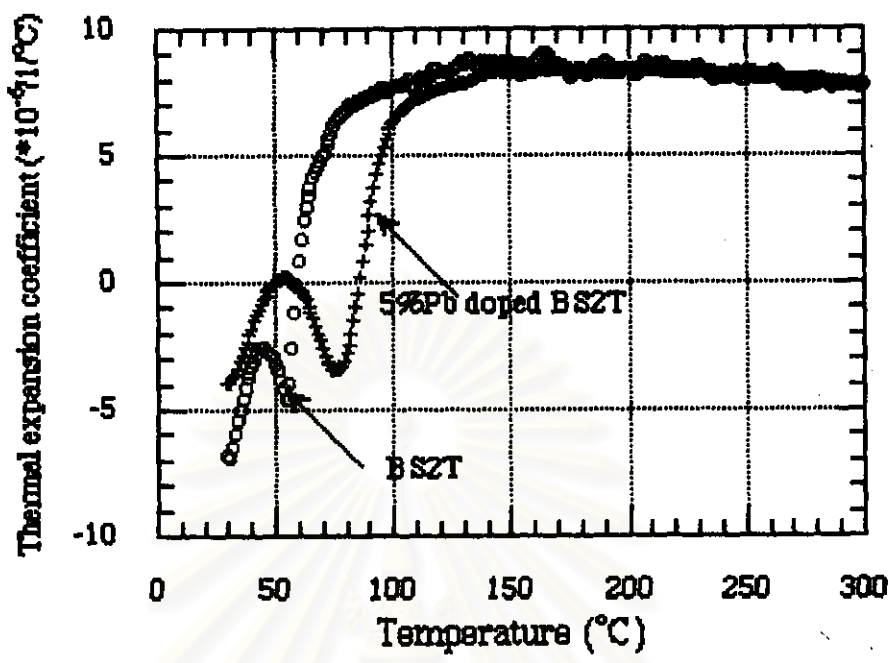


Fig. 4.10 Change in thermal expansion coefficient of $0.95\text{Ba}_{0.8}\text{Sr}_{0.2}\text{TiO}_3 - 0.05\text{PbTiO}_3$ and $0.90\text{Ba}_{0.8}\text{Sr}_{0.2}\text{TiO}_3 - 0.10\text{PbTiO}_3$ sintered at 1350°C and soaked 30 minutes.

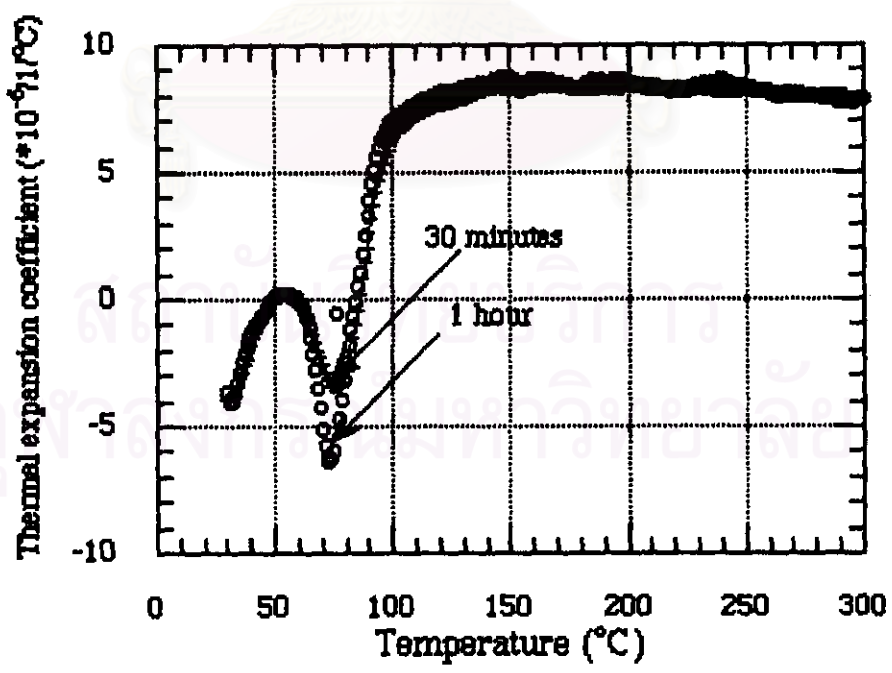


Fig 4.11 Change in thermal expansion coefficient of $0.95\text{Ba}_{0.8}\text{Sr}_{0.2}\text{TiO}_3 - 0.05\text{PbTiO}_3$ sintered at 1350°C with different soaking time.

In conclusion, the effect of Pb-dopant on the transition temperature of $\text{Ba}_{0.8}\text{Sr}_{0.2}\text{TiO}_3$ has much more significance than that of sintering temperature and soaking time. But the effect of soaking time on C.O.E. value has much more significance than that of composition and sintering temperature.

Table 13 Thermal expansion coefficient above T_c of $(1-x)\text{Ba}_{0.8}\text{Sr}_{0.2}\text{TiO}_3-x\text{PbTiO}_3$ as a function of composition, sintering temperature and soaking time.

Composition (x)	Sintering temperature ($^{\circ}\text{C}$)	C.O.E. above T_c ($*10^{-6}/1^{\circ}\text{C}$)
0	1350	8.2
0.05	1320	8.2
	1350	8.0
0.10	1320	8.1
	1350	8.1

Composition (x)	Soaking Time	C.O.E. above T_c ($*10^{-6}/1^{\circ}\text{C}$)
0.05	30 minutes	8.0
	1 hour	8.3

4.4 Dielectric properties of $(\text{Ba}_{0.75}\text{Sr}_{0.25}\text{Ca}_{0.02})\text{TiO}_3$ and $(\text{Ba}_{0.80}\text{Sr}_{0.20})$ $(\text{Zr}_{0.05}\text{Ti}_{0.95})\text{O}_3$

BST has not only the high dielectric constant but also high variation of dielectric constant with temperature. The dielectric can be modified to broaden the dielectric peak for use in a wide temperature range.

The past researches had been studied about the addition of calcium to barium titanate. They found that calcium lowered the room temperature dielectric constant and shifted the second phase transition to lower temperature. In addition, they found

that zirconia increased the second transition temperature in BaTiO_3 . Therefore, calcium and zirconia are considered to be the dopants in order to suppress and distribute the transition peak. In this experiment, the effects of calcium and zirconia on the dielectric properties are studied.

Fig 4.12 shows the dielectric constant and the dissipation factor as a function of temperature for $(\text{Ba}_{0.75}\text{Sr}_{0.23}\text{Ca}_{0.02})\text{TiO}_3$ sintered at 1350°C and soaked 30 minutes. The graph of dielectric constant vs. temperature shows a Curie point at 65°C . Below the Curie point the dielectric constant increases as the temperature increases and at the Curie point the dielectric constant is highest as this point has the highest polarizability. Above the Curie point the dielectric constant falls since the ferroelectric phase of $(\text{Ba}_{0.75}\text{Sr}_{0.23}\text{Ca}_{0.02})\text{TiO}_3$ has changed to a paraelectric phase that is similar to undoped $\text{Ba}_{0.8}\text{Sr}_{0.2}\text{TiO}_3$.

At room temperature, the dielectric constant at 1 kHz is about 2600 and decreases to 2150, 2000 and 1900 at frequencies of 10, 100 and 1000 kHz, respectively. In addition, the maximum dielectric constant at lower frequency is higher than at higher frequency.

Fig 4.12 shows the effect of frequency and temperature on the dissipation factor of $(\text{Ba}_{0.75}\text{Sr}_{0.23}\text{Ca}_{0.02})\text{TiO}_3$. Below the Curie point, the dissipation factor decreases as the temperature increases. This is due to domain wall motion in the ferroelectric region. Above the Curie temperature the dissipation factor tends to increase because the effect of conductivity.

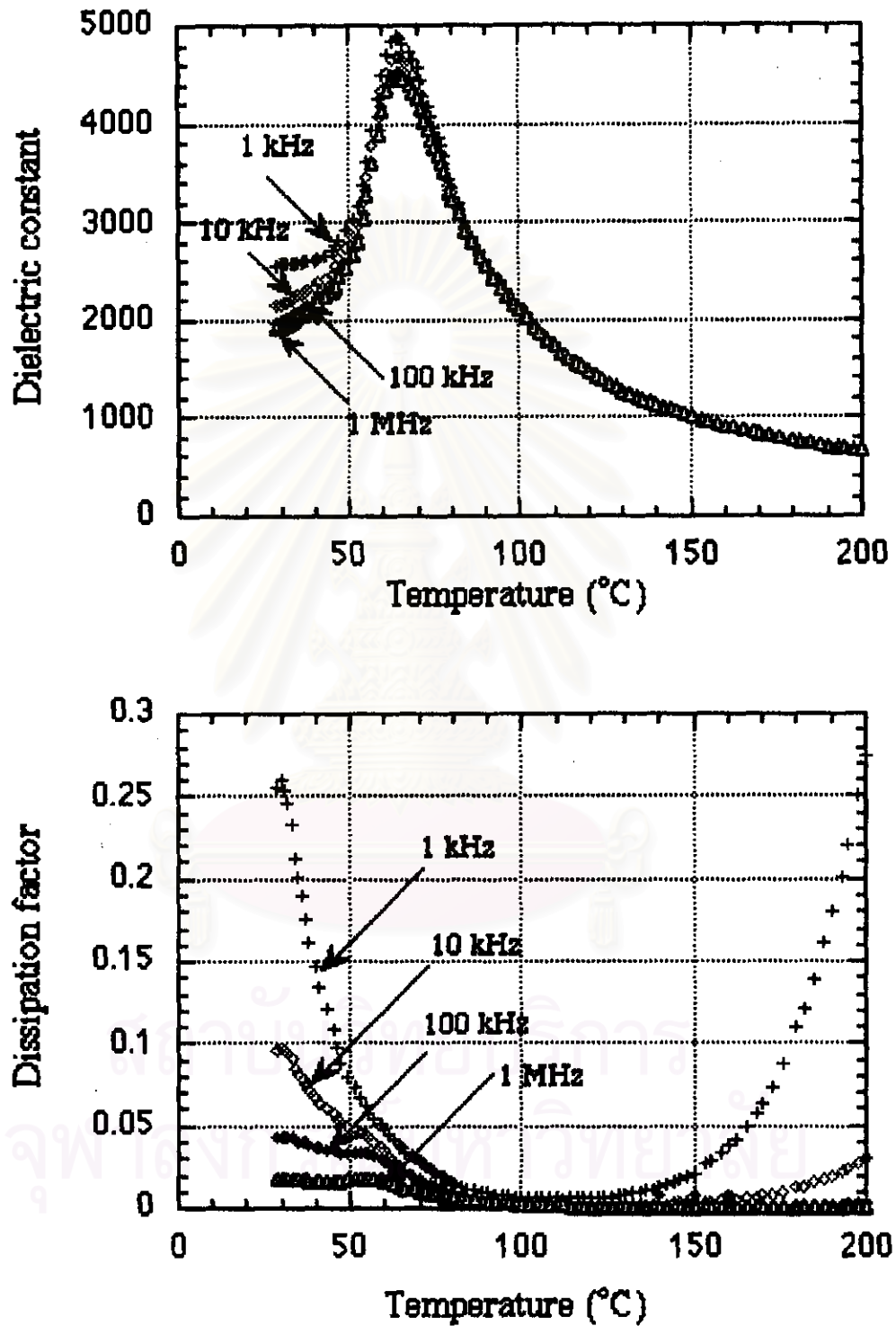


Fig. 4.12 Change in dielectric constants and the dissipation factors of $(\text{Ba}_{0.75}\text{Sr}_{0.23}\text{Ca}_{0.02})\text{TiO}_3$ sintered at 1350°C at different frequencies.

Fig 4.13 shows the dielectric constant and dissipation factor as a function of temperature for $(\text{Ba}_{0.8}\text{Sr}_{0.2})(\text{Zr}_{0.05}\text{Ti}_{0.95})\text{O}_3$ sintered at 1350°C for 30 minutes. The graph of dielectric constant vs. temperature shows a Curie point at about 60°C . From room temperature, the dielectric constant decreases as the temperature increases that results from the effect of Zr, which shifts the second phase transition to a higher temperature. Then the dielectric constant increases as the temperature increases until the Curie point. Above the Curie point the dielectric constant decreases since the ferroelectric phase changes to a paraelectric phase. This plot also shows an effect of frequency on the dielectric constant of $(\text{Ba}_{0.8}\text{Sr}_{0.2})(\text{Zr}_{0.05}\text{Ti}_{0.95})\text{O}_3$. The dielectric constant at the Curie temperature is about 2250 at a frequency of 1 kHz and decreases to 1950, 1900 and 1850 at a frequencies of 10, 100 and 1000 kHz, respectively. The dielectric constant decreases as the frequency increases because at the higher frequency the movement of domain wall reduce.

The effects of frequency and temperature on the dissipation factor of $(\text{Ba}_{0.8}\text{Sr}_{0.2})(\text{Zr}_{0.05}\text{Ti}_{0.95})\text{O}_3$ also shows in Fig 4.14. At room temperature, not only the dielectric constant is high but the dissipation factor. This is disadvantageous so that the range is not suitable for utilization. The dissipation factor decreases as the temperature increases and then, increases as the temperature is higher than 130°C because of the conductivity.

Fig 4.14 shows the effect of dopant on the dielectric constant and dissipation factor of BST sintered at 1350°C and soaked for 30 minutes at a frequency of 10 kHz as a function of temperature. The graph of dielectric constant vs. temperature shows a little change of Curie point of $(\text{Ba}_{0.75}\text{Sr}_{0.23}\text{Ca}_{0.02})\text{TiO}_3$ and $(\text{Ba}_{0.8}\text{Sr}_{0.2})(\text{Zr}_{0.05}\text{Ti}_{0.95})\text{O}_3$ which is approximately 2°C - 5°C below that of undoped $\text{Ba}_{0.8}\text{Sr}_{0.2}\text{TiO}_3$. The maximum dielectric constant decreases from 13000 to 5000 for $(\text{Ba}_{0.75}\text{Sr}_{0.23}\text{Ca}_{0.02})$

TiO_3 and 2000 for $(\text{Ba}_{0.8}\text{Sr}_{0.2})(\text{Zr}_{0.05}\text{Ti}_{0.95})\text{O}_3$. Ca doped BST broadens the dielectric peak and decreases the dielectric constant at all temperature but it does not affect to the Curie point.

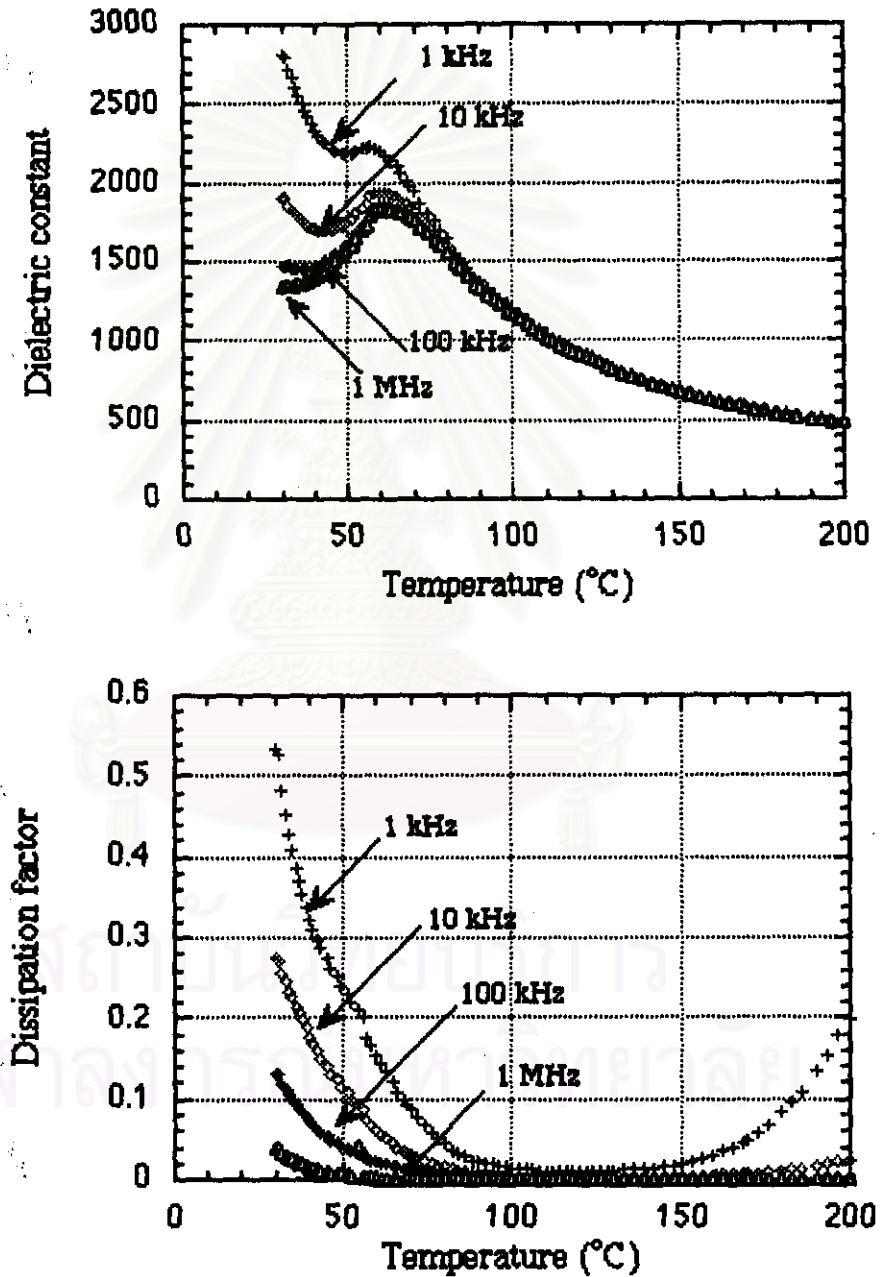


Fig. 4.13 Change in dielectric constants and the dissipation factors of $(\text{Ba}_{0.8}\text{Sr}_{0.2})(\text{Zr}_{0.05}\text{Ti}_{0.95})\text{TiO}_3$ sintered at 1350°C at different frequencies.

The dielectric peak of $(\text{Ba}_{0.8}\text{Sr}_{0.2})(\text{Zr}_{0.05}\text{Ti}_{0.95})\text{O}_3$ composition is suppressed. Its dielectric constant is lower than that of $(\text{Ba}_{0.75}\text{Sr}_{0.23}\text{Ca}_{0.02})\text{TiO}_3$. Similarly, both of them are lower than that of undoped BST. In addition, the dissipation factors of Ca doped BST and Zr doped BST are higher than that of undoped BST (about 0.095 for Ca doped, 0.27 for Zr doped and 0.04 for undoped BST).

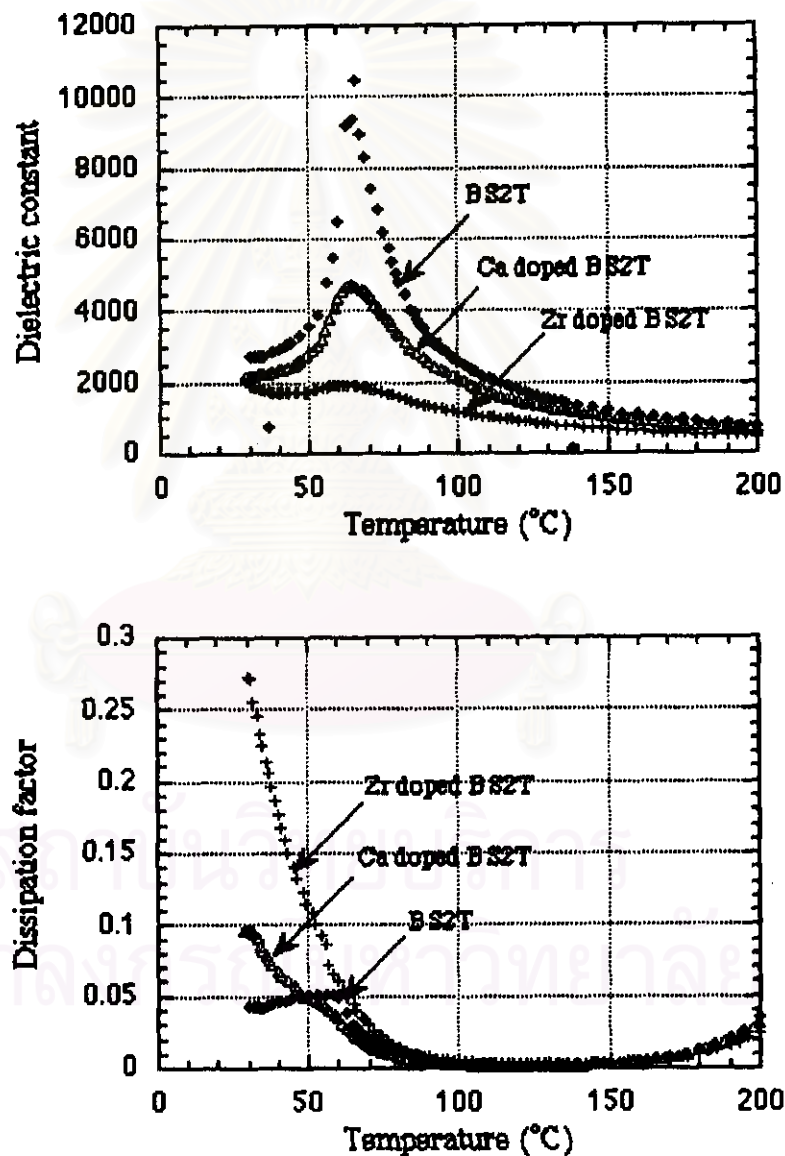


Fig. 4.14 Change in dielectric constant and the dissipation factor of Ca doped BST and Zr doped BST with sintered at 1350°C and soaked 30 minutes for 10 kHz.